Feasibility of CO₂ Extraction from Seawater and Simultaneous Hydrogen Gas Generation Using a Novel and Robust Electrolytic Cation Exchange Module Based on Continuous Electrodeionization Technology

Heather D. Willauer,*,[†] Felice DiMascio,[‡] Dennis R. Hardy,[§] and Frederick W. Williams[‖]

[†]Materials Science & Technology Division and [‖]Chemistry Division, Naval Research Laboratory, 4555 Overlook Avenue, SW, Washington, D.C. 20375, United States

[‡]Office of Naval Research, 875 North Randolph Street, Arlington, Virginia 22203, United States

[§]Nova Research Inc., 1900 Elkin Street, Alexandria, Virginia 22308, United States

ABSTRACT: A novel, robust, and innovative electrolytic cation exchange process has been used to efficiently extract large quantities of CO_2 in the form of bicarbonate and carbonate from natural seawater, and to simultaneously produce H_2 gas in quantities and ratios intended for possible future production of hydrocarbons. This indirect approach acidifies seawater by using the protons electrolytically produced by electrolysis at the anode. Electrons concurrently produced with these protons are subsequently consumed at the cathode forming hydrogen gas. The ability to degas and recover 92% $[CO_2]_T$ from natural seawater was demonstrated. The potential detrimental effects of mineral deposits on the module's electrode surfaces were successfully mitigated by cyclically changing the module electrode's polarity. This feasibility study marks the first time that CO_2 has been successfully extracted on a continuous basis from natural seawater. In addition, there is no energy or economic penalty to extract CO_2 from the seawater matrix, above the energy needed to produce hydrogen.

■ INTRODUCTION

Finding solutions to minimize the anthropogenic levels of carbon dioxide (CO_2) in the atmosphere has led to extensive research efforts in the development of technologies specifically designed to capture CO_2 from concentrated sources such as fossil fuel burning power plants, cement plants, and refineries.[1,2] However, these sources are responsible for only roughly half of all anthropogenic carbon dioxide emissions.[1] The other half may be attributed to the transportation industry. These latter sources are mobile in nature, produce relatively low concentrations of CO_2 on an individual basis, and are thus difficult to capture on an individual basis.[1] Therefore, a more general approach to CO_2 removal from the environment may be needed to minimize anthropogenic CO_2 effects.

In the environment, the CO_2 in the atmosphere is in constant equilibrium with the ocean, so as anthropogenic CO_2 increases in the atmosphere, the world's oceans absorb more and more CO_2 as carbonic acid. Carbonic acid is in equilibrium with carbonate and bicarbonate species which are primarily responsible for buffering and maintaining the oceans' pH.[3,4] At seawater pH of less than or equal to 6, the dissolved bicarbonate and carbonate reequilibrate to CO_2 gas. This process has been the basis for standard ocean CO_2 measurements for over 25 years.[5] Currently the total carbon dioxide concentration of the world's oceans is about 100 mg/L minimum at all depths, latitudes, and longitudes. Approximately 2−3% of this CO_2 is in the form of a dissolved gas, and the remaining 97−98% is in a chemically bound state as bicarbonate and carbonate.[3,4] Given the total ocean volume of about 1.3×10^{21} L, this means that the CO_2 content of the oceans is 1.3×10^5 gigatons (GT) compared to 8.0×10^2 GT

in the entire atmosphere. Thus, the oceans are about 175 times greater than the atmosphere as a total carbon reservoir. When the CO_2 concentration of the ocean is compared to its concentration in the atmosphere on a weight per volume basis (w/v) (100 mg/L), CO_2 in seawater is about 140 times more concentrated than in air (0.77 mg/L).[6] The CO_2 in stack gases is about 385 times more concentrated than that found in the atmosphere on a v/v or w/v basis (about 296 mg/L (w/v) for typical stack gas vs about 0.77 mg/L in air (w/v)).[1] In addition, comparing the high seawater concentration on a w/v basis (about 100 mg/L) to that of stack gases (about 300 mg/L) indicates that this is another powerful reason to consider ocean extraction of CO_2 rather than air extraction of this important anthropogenic gas.[7−9]

Energy efficient processes to take advantage of the higher w/v concentration of CO_2 in seawater would be advantageous from several environmental perspectives. First, CO_2 would be indirectly removed from the atmosphere. Second, the effluent seawater medium generated would be capable of absorbing more CO_2 from the atmosphere without further effect on ocean alkalinity. Additionally, the pure CO_2 removed from the ocean would eliminate costly energy intensive regeneration steps needed for processes to recover CO_2 by standard alkaline absorption processes from concentrated sources of CO_2.[1,2] This recovered CO_2 from seawater could be directly used for a growing number of processes seeking to increase product

Center Compartment Reactions:

$2NaCl + 2H^+ \rightarrow 2HCl + 2Na^+$

$2NaHCO_3 + 2H^+ \rightarrow 2H_2CO_3 + 2Na^+$

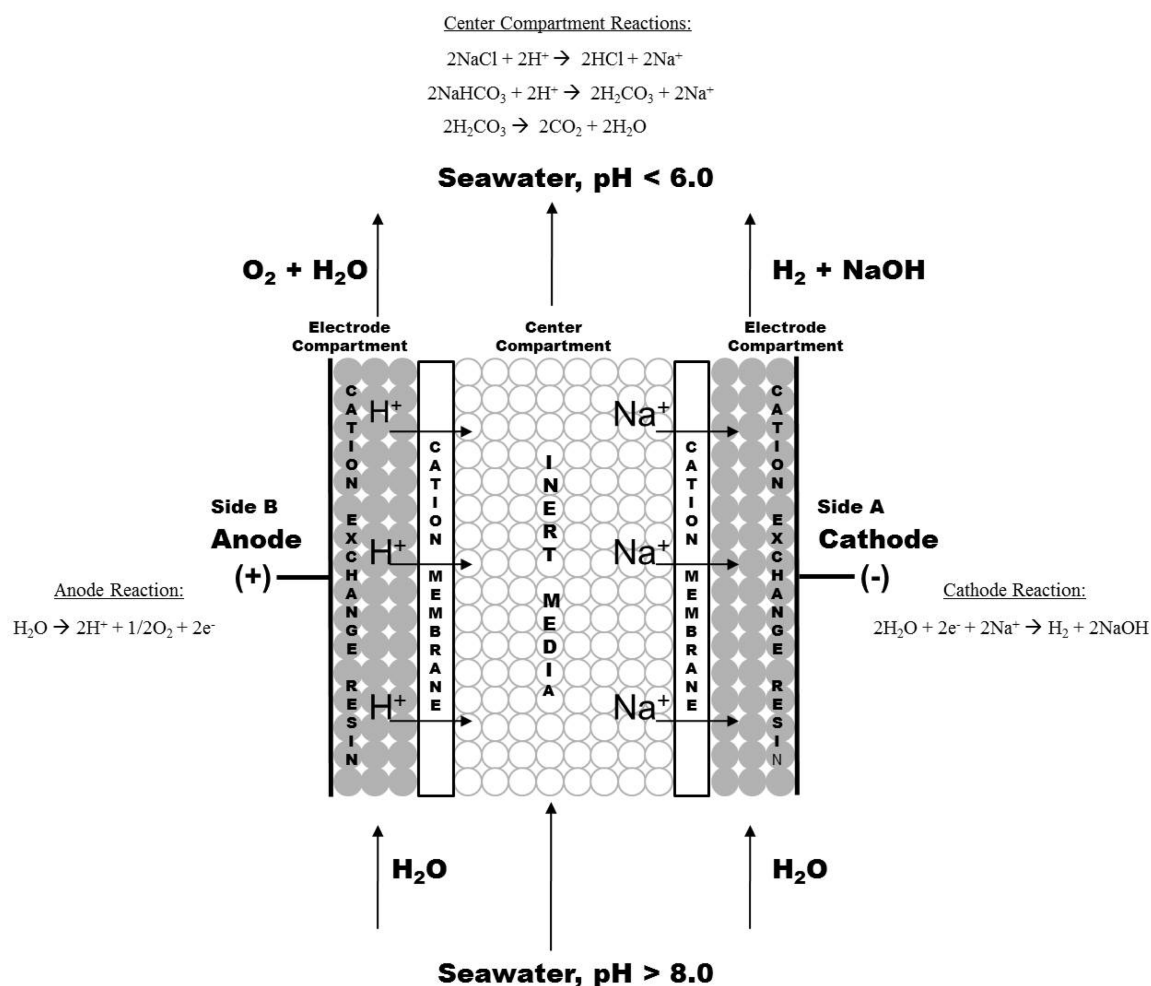$2H_2CO_3 \rightarrow 2CO_2 + 2H_2O$

Seawater, pH < 6.0

Figure 1. Schematic of E-CEM. Positive ions travel through solution from the electrode functioning as the anode (as pictured side B) to the electrode functioning as the cathode (as pictured side A). Module is pictured operating as polarity A.

efficiencies and reduce their overall carbon footprint. These processes include enhanced biological carbon fixation,[1,10−12] new strategies involving CO_2 in low temperature solidification processes,[13] and thermal catalytic processes to produce energy rich hydrocarbons.[14−18]

Currently, bipolar membrane electrodialysis (BPMED) for acidification of seawater is the only reported comparable alternative electrochemical approach for removal of CO_2 from seawater.[19] Though an electrochemical energy consumption of 242 kJ/mol CO_2 from synthetic seawater is reported for that method,[19] many challenges remain to implementing BPMED technology using natural seawater that include the following: (1) the use of monopolar ion exchange membranes prevents the ability of the BPMED method to address mineral deposition on the electrode surface resulting from precipitation of calcium and magnesium from seawater, (2) the bilayer membrane technology has been shown to degrade over time, (3) the use and storage of electrode solutions containing strong acid (0.2 M H_2SO_4/0.25 M Na_2SO_4) is necessary for the method to operate, (4) testing of the BPMED process using natural seawater systems that represent actual naturally occurring open ocean carbonate/bicarbonate buffer systems was never undertaken, and (5) the method shows only 59% recovery efficiency of $[CO_2]_T$ from synthetic seawater which represents a far easier recovery system than does naturally occurring seawater.[8,9] Finally, the BPMED technology is not

capable of addressing the higher energy needs to obtain H_2 from the cathode reaction. Therefore, additional water electrolysis equipment is needed for production of hydrogen for use in the thermochemical reduction of carbon dioxide to hydrocarbons.

In this paper we describe the scale-up, feasibility, and continuous operation of a three-chambered electrolytic cation exchange module (E-CEM) approach and its integration into a skid platform that addresses these challenges. This E-CEM has been scaled-up from processing 700 mL/min (in the laboratory) to processing 1900 mL/min of natural Key West (Florida) seawater (in a marine environment). In previous laboratory scale work, we referred to these modules as electrochemical acidification cells.[8,9]

As natural Key West (KW) seawater is pumped through the center chamber in a continuous flow process as shown in Figure 1, the bicarbonate and carbonate in the seawater are reequilibrated to carbonic acid by the addition of protons as shown in eq 1.

$$HCO_3^- + CO_3^{2-} + H^+ \rightleftarrows H_2CO_3 \rightleftarrows H_2O + CO_2(g)\uparrow \tag{1}$$
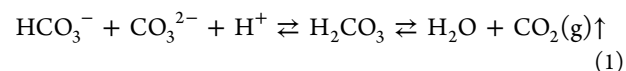
Seawater's salinity is approximately 35 g/L and is primarily attributed to sodium chloride. The total chloride content in seawater is about 240 times greater than the targeted bicarbonate and carbonate ions.[20] Therefore, the reactions
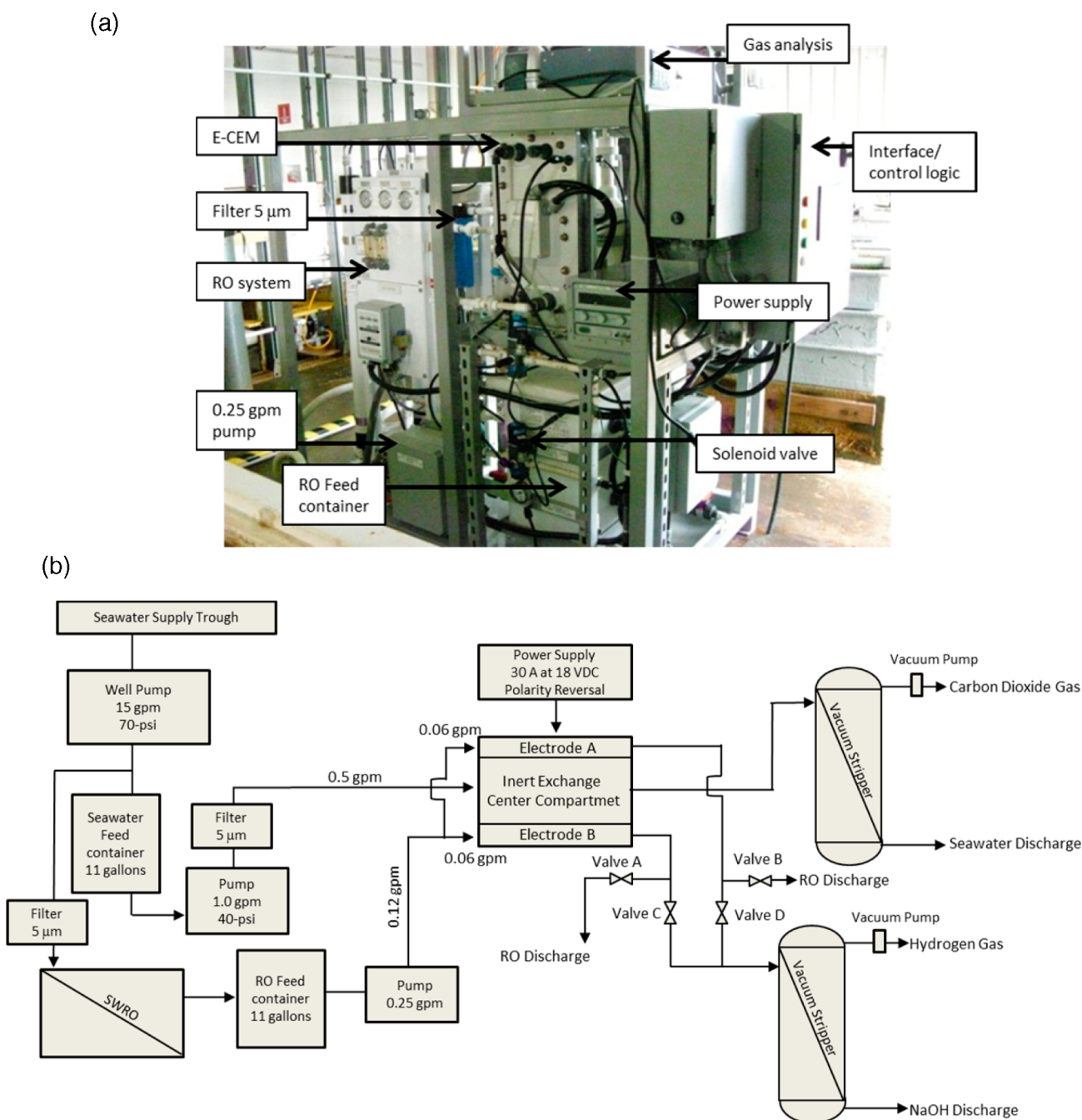
(a)

(b)

Figure 2. (a) Labeled photograph of experimental setup. (b) Block diagram of the experimental setup.

within the E-CEM may be simplified as shown in Figure 1 when sodium chloride (NaCl) is used to represent seawater and HCl is used to represent the acidified effluent seawater. When direct current is applied to the cell, H^+ and O_2 gas are produced at the anode by oxidation of the anolyte water. The amount of H^+ generated by the anode is proportional to the applied electrical current, which follows Faraday's law. The anode and cathode reactions to theoretically determine the amount of H^+, OH^-, H_2, and O_2 produced per amp per second current passed through the electrodes has been previously detailed by Willauer et al.[8,9] The O_2 gas is flushed from the anode compartment with the flow of the anolyte (deionized water). The H^+ ions are driven from the surface of the anode, through the cation-permeable membrane, and into the center compartment where they replace the Na^+ in the flowing

seawater. This causes the effluent seawater to be acidified without the need for any additional chemicals. In this process, the CO_2 gas is subsequently vacuum stripped, producing a stream of essentially pure CO_2 gas with traces of water vapor and air.

The Na^+ ions in the center compartment are passed through the membrane closest to the cathode to produce primarily sodium hydroxide and H_2 gas in the cathode compartment. The NaOH and H_2 gas are continuously flushed from the cathode compartment with the flow of the catholyte (deionized water). The acidified seawater is recombined with the basified solution from the cathode compartment to return the effluent seawater to its original pH as measured by a pH meter. The simultaneous production of H_2 at the cathode in molar quantities needed for thermal catalytic processes to make

hydrocarbons from CO_2 is a unique feature of this process. This feature of the process utilizes the simultaneous production of electrons needed for hydrogen gas production with the production of protons for acidification of seawater. In other words, for each unit of electricity consumed to make the hydrogen gas at the cathode, the protons are used to acidify the seawater below pH 6 in the central compartment. All commercial and laboratory water electrolysis units to date have disposed of the protons produced by discharging them with the anode waste. In this way, the E-CEM process makes the electrical energy needs for CO_2 production from seawater an energetically free byproduct of the hydrogen gas production.

■ EXPERIMENTAL METHODOLOGY

Electrolytic Cation Exchange Module (E-CEM). Figure 1 shows the modified (patent pending) E-CEM and a schematic of the inside of the module configuration. A standard commercially available electrodeionization cell (Ionpure LX-X Module) was modified to function as an electrolytic cation exchange module for this work on feasibility and scalability. The major components of the E-CEM include a center compartment, electrode compartments (cathode and anode capable of reversing polarities), and cation-permeable membranes which separate the three compartments. Polyethylene extruded cation-permeable heterogeneous membrane incorporates cross-linked polymer with sulfonic acid groups attached. The acid functionality provides discrete channels for cations to migrate through the polymer matrix while blocking the passage of anions. Inert plastic particles were used in the center compartment to serve as a support structure for the membranes. In this central compartment, the ions (Na^+/H^+) exchange in the liquid phase. In addition, Figure 1 shows that the electrode compartments contain strong acid cation exchange resin (Rohm & Haas IR-120). The resin and membranes used in this process are typically used for years in commercial water treatment electrolysis processes. Our water filtration and current densities are well within the specifications of all products used to construct the module. After 3 years, we have not seen any degradation or deterioration of the resin or membranes used to construct the module. The anode and cathode titanium electrodes were coated with platinum and had an electrode active area of 497 cm^2.

In this continuous flow process, seawater was passed through the center compartment of the module shown in Figure 1 at a flow rate of 0.5 gal/min (1900 mL/min), while freshwater was passed through the anode and cathode compartments each at 0.06 gal/min (230 mL/min). Direct current (dc) was used to produce H^+ ions, O_2, and electrons at the anode. These H^+ ions migrated from the surface of the anode, through the cation-permeable membrane, and into the center compartment where they replaced the Na^+ ions in the seawater to acidify the seawater. The Na^+ ions were transferred through the membrane closest to the cathode and removed from the seawater. Simultaneously at the cathode OH^- ions and H_2 are produced and electrons are consumed. The positive ions removed from the seawater (sodium being at the highest concentration) provide electrical neutrality in the cathode compartment to form a basic solution composed primarily of sodium hydroxide. The freshwater used in the module was produced from the natural Key West (KW) seawater using a reverse osmosis system (RO). The freshwater had a conductivity of less than 200 μS/cm and measured approximately pH 7. Magnesium and calcium ions also migrate to the cathode compartment and

produce scale on the cathode over time. The effects of this scale are mitigated by cyclically reversing the module's polarity.

Carbon Capture Skid and Procedure. Since natural Key West seawater was used, the work was performed at the Naval Research Laboratory's Corrosion Laboratory at Key West, FL, to evaluate the E-CEM's performance. The module was incorporated into a portable skid along with an RO unit, power supply, pumps, carbon dioxide recovery system, hydrogen gas vacuum tower, and gas analyzer to form a carbon capture system, all operated by a control logic capable of maintaining operation safely on a continual basis. Figure 2 shows a labeled photograph and a block diagram of the CO_2 capture skid. Seawater was supplied to the skid by an in-house 40 psi supply line. The water was filtered by two spin-down filters in series (100 and 30 μm). After filtration, a portion of the seawater was sent to an 11 gal high density polyethylene container that functions as the seawater feed container. Before the seawater in the seawater feed tank was fed to the center compartment of the E-CEM at 0.5 gal/min (1900 mL/min), it was pumped through a 5 μm filter cartridge. The other portion of the seawater supply was fed through a 5 μm filter cartridge to the RO system for processing. The RO system was an EPRO-1000SW from Crane Environmental, Inc. (Venice, FL), that is capable of producing 0.7 gal/min (1000 gal/day) of permeate (freshwater quality from seawater at a conductivity of approximately 200 μS/cm). This water was stored in an 11 gal polyethylene container that is specified as the RO feed container (Figure 2). This water was the feedwater to the electrode compartments of the E-CEM at a total flow rate of 0.12 gal/min (460 mL/min). The flow was split within the E-CEM resulting in electrode compartment flow rates of 0.06 gal/min (230 mL/min) to each electrode compartment.

A Mastech HY3030EX 0−30 A, 0−30 V high-current, regulated dc power supply was used to supply the current to the E-CEM electrodes. The seawater pH changed as a function of applied current to the E-CEM. Effluent seawater pH was monitored continuously using a standard combination electrode as it exited the center compartment of the module. Vision 290 Unitronics hardware and software were used to control the system components (RO, E-CEM, well pump, vacuum towers, vacuum pumps, solenoid valves, and power supply) so that they operated and functioned together as an integrated unit on a continual basis, with limited operator control required. The CO_2 gas from the effluent acidified seawater flowing at 0.5 gal/min was vacuum stripped using a commercial membrane contactor (Liqui-Cel 2.5 × 8 polyethylene hollow fiber membrane contactor (Membrana-Charlotte). The $[CO_2]_T$ content of the acidified effluent seawater was measured by coulometry (UIC Inc., Joliet, IL) after contact with the membrane contactor to determine the efficiency of the extraction method.[5] The $[CO_2]_T$ content of the natural Key West seawater before acidification was measured to be approximately 100 mg/L. Simultaneously, a standard purpose-built hydrogen gas vacuum tower processed the water from the cathode compartment of the module as it liberated H_2 gas. The H_2 gas was measured qualitatively throughout the operation by a standard Honeywell gas analyzer (7866 digital gas analyzer), as was the CO_2.

■ RESULTS AND DISCUSSION

The objective of this study was to transition the technology from the laboratory scale to an actual marine environment using natural seawater for the purpose of scaling up, integrating,

and demonstrating the feasibility of the technology. NRL—Key West Corrosion Laboratory (Key West, FL) provided a marine environment that had an abundant supply of unpolluted and undisturbed natural seawater. As a result, sample conditions that would be encountered in an actual open ocean process could be utilized. In this environment, we were able to use the technology to produce CO_2 and H_2 in quantities far above those achievable at the laboratory scale.

To overcome a major challenge of mineral deposition on the electrode surface not anticipated and not possible using the current BPMED design,[19] polarity switching was designed into our system to provide electrode regeneration at regular intervals, called polarity cycles (described below).[21,22] This regeneration is needed to prevent module degradation from the effects of calcium and magnesium precipitation in the high pH environment of the cathode. In this initial study of the system and module performance, the effluent natural seawater pH, current, voltage, and resistance were measured as a function of time during a polarity cycle. The electrode compartments are defined as side A and side B (Figure 1). Polarity A and polarity B designate the electrode compartment (side A or side B) that is functioning as the cathode during the polarity cycle. These profiles establish (1) the time it takes to acidify the seawater as a function of current density, (2) the performance of both electrodes over time as they cyclically change between functioning as the cathode and functioning as the anode, (3) the time it takes to see signs of degradation in module performance (degradation is defined as an increase in electrical resistance most likely from mineral deposition on the electrode surface and defines the length of a polarity cycle), (4) the total CO_2 recovery as a function of pH, and (5) H_2 production at the cathode. At this scale these profiles are key in determining overall process efficiencies and identifying areas where system and module performance can be improved for future large scale process designs.

Results are presented in Figure 3 for four consecutive polarity cycles while the module was operated at the maximum design current of 30 A and processing the maximum seawater flow design of 0.5 gal/min. At these design specifications, production of feedstock ratios of 3:1, H_2 to CO_2, from seawater were targeted. This equates to approximately 0.003−0.004

mol/min CO_2 (78−100% recovery efficiencies from seawater) and 0.0093 mol/min H_2 (100% recovery efficiencies from water). The first two consecutive cycles were 59 min each with an 86 s flush period between the cycles. The next two consecutive cycles ran for 40 min each with a longer flush period of 157 s. During the flush cycle RO water was used to wash the excess H_2, NaOH, O_2, and H^+ from the electrode compartments before the polarity was reversed. Figure 3 compares the pH profiles of the four polarity cycles as a function of time. Effluent seawater samples were collected every 5 min and their pH was measured. The initial pH of the influent Key West seawater was 8.04 ± 0.02. Figure 3 shows that, after approximately 19 min have passed in all four cycles, the pH of the effluent seawater dropped below 6.00. This time is a function of the strong acid cation exchange resin volume (215 cm^3) in the electrode compartments (Figure 1) and the amount of applied current. After 25 min the pH of the effluent seawater from both cycles measured below 3. Figure 3 shows that both cycles provide a similar pH profile as a function of time. This verifies the performance of both electrodes as they cyclically change between functioning as the cathode and functioning as the anode. In addition, it indicates the packing density of the ion exchange material is uniform in the electrode compartments.

Figure 4 shows the pH profiles for two consecutive 40 min polarity cycles at 30 A. While Figure 3 was a side-by-side

Figure 4. A pH profile in succession of two consecutive 40 min polarity cycles at 30 A (612 A/m^2 current density) as a function of time: (■) 40 min cycle, polarity B; 40 min cycle, polarity A (□).

comparison of four consecutive cycles as a function of time, Figure 4 illustrates the third and fourth consecutive cycles along with the flush cycle in succession. Figure 4 clearly illustrates that once a cycle ends, the electrode compartments are flushed, the polarity is switched, and a new cycle begins, the pH of the effluent returns to that of the influent. This is critical because equilibrium conditions of the cation exchange material in the module's electrode compartments must be reestablished upon changing the polarity of the module. When the polarity of the module is reversed, the H^+ ions generated on the electrode that is now functioning as the anode exchange on the resin and release Na^+ ions. The Na^+ ions then migrate through the cation exchange membrane and into the center compartment. The migrating Na^+ ions pass through the cation exchange membrane at the electrode now acting as the cathode and exchange on the resin to convert all the resin in that
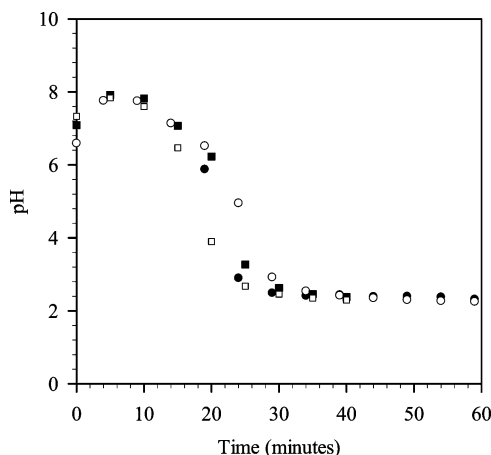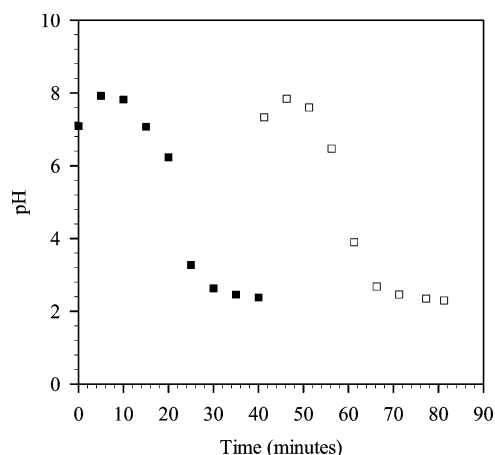
Figure 3. A pH profile comparison of four polarity cycles at 30 A (612 A/m^2 current density) as a function of time: (●) 59 min cycle, polarity B; (○) 59 min cycle, polarity A; (■) 40 min cycle, polarity B; (□) 40 min cycle, polarity A.

compartment to the sodium form. Equilibrium conditions are reestablished during the polarity cycle when all the resin in the compartment now acting as the anode is regenerated back into the hydrogen form and all the resin in the cathode is regenerated back into the sodium form. Figure 3 shows that at 19 min and 30 A for all four cycles, the ion exchange material in the electrode compartments reaches equilibrium or a level of full regeneration, allowing more H^+ ions to pass through the membrane closest to the anode to acidify the seawater. As a result, the pH of the effluent seawater drops. Since the amount of H^+ ions generated from the oxidation of water on the electrode functioning as the anode is proportional to the applied electrical current, the higher the current the faster the module will reach a state of equilibrium. These data provide important insights into the future design of the module. The equilibrium value may be reduced by changing the electrode compartment configuration and reducing or changing the ion exchange material. Design efforts can also be directed toward maintaining a constant effluent seawater pH throughout the consecutive polarity cycles. All of these insights are being pursued in future module designs. As a result of scaling-up and integrating the technology into a carbon capture skid, we have a versatile platform to test, evaluate, demonstrate, and compare all the future module designs under similar marine environmental conditions.

Figure 5 is a side-by-side comparison of pH profiles when the module was operating in the same polarity configuration at
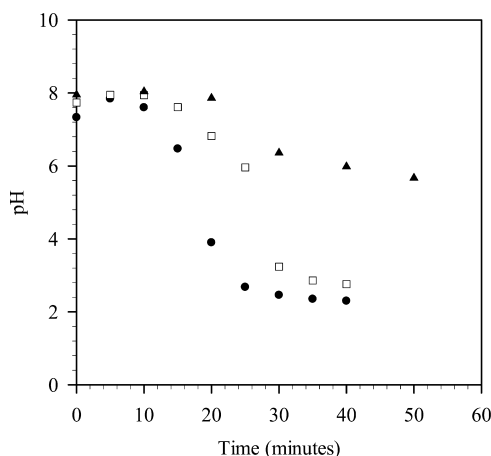

Figure 5. A pH profile comparison for three polarity cycles measured at different applied cell currents: (●) 30 A (612 A/m² current density), 40 min cycle, polarity B; (□) 20 A (408 A/m² current density), 40 min cycle, polarity B; and (▲) 10 A (204 A/m² current density), 45 min cycle, polarity B.

different applied module currents of 30, 20, and 10 A. When the applied module current was reduced from 30 to 20 A, it took approximately 25 min for the pH of the effluent seawater to drop below 6.0 and 35 min to fall below pH 3. At 10 A, the time for seawater pH to fall below 6.0 increased to 40 min and a seawater pH below 3 was never achieved. The applied module current of 10 A is comparable to the theoretically calculated minimum applied current of 7 A needed in these experiments to lower the seawater pH to less than 6.0 and completely convert HCO_3^- to H_2CO_3 when equilibrium is reached.[8,9] Figure 5 shows that similar pH profiles are achieved for a defined applied module current as a function of time and serves

to illustrate that seawater pH is proportional to the applied module current over time.

The increase in electrical resistance as a function of time is a sign of mineral deposition on the cathode. Scaling (mineral deposits) takes place at the high-pH surface of the cathode (Figure 1). The formation of mineral deposits decreases the active electrode surface area causing an increase in the electrical resistance across the entire module. This in turn leads to an increase in power consumption by increasing the voltage and could cause a pressure drop in the electrode compartment functioning as the cathode. By cyclically reversing the polarity of the module's electrodes, the mineral deposits will be reduced on the electrode that was operating as the cathode in the previous cycle. The change in polarity causes the minerals (scaling) to dissociate from the electrode surface. Polarity reversal is a common practice in electrodialysis reversal (EDR) processes that are used to desalinate brackish ground and surface waters.[21,22] Evaluation of how well polarity reversal of the module minimized mineral deposits on the electrode functioning as the cathode was one of the key objectives of this test series.

Figure 6 is a plot of electrical resistance (voltage divided by amperage) as a function of time for the two 59 min consecutive
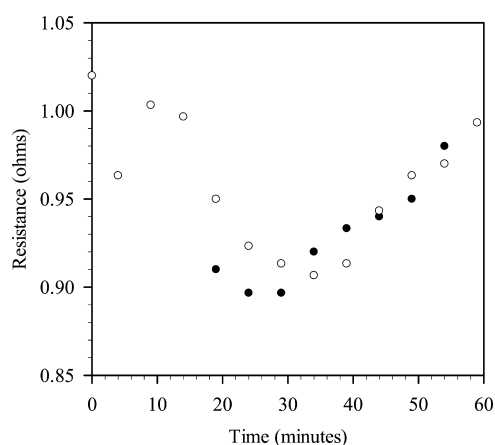

Figure 6. Electrical resistance comparison of two consecutive 59 min polarity cycles at 30 A (612 A/m² current density) as a function of time: (●) polarity B and (○)polarity A.

polarity cycles at 30 A. Comparing both cycles shows that the resistance decreases by approximately 11% over the first 29 min of operation. During the remaining 30 min of both cycles the resistance increases by 10−11%. Figure 7 illustrates the 40 min consecutive polarity cycles in succession. During each cycle the electrical resistance decreases by approximately 10−11% in the first 25 min and then increases to 0.91 ohm over the remaining 15 min. Figure 7 also shows that, once the electrode compartments were flushed for 86 s and the polarity was reversed, the electrical resistance of the module at the start of the fourth cycle was as high as 1.0 ohm. This is explained by the conductivity of the ion exchange resin in the electrode compartments upon polarity reversal. When the polarity is reversed, the ion exchange resin in the electrode compartment functioning as the anode is in the sodium form. This form of the resin is less conductive, and as a result more voltage to the module is needed to maintain the current. The voltage is reduced as equilibrium conditions in the module are reestablished. At the same time minerals are dissociated from
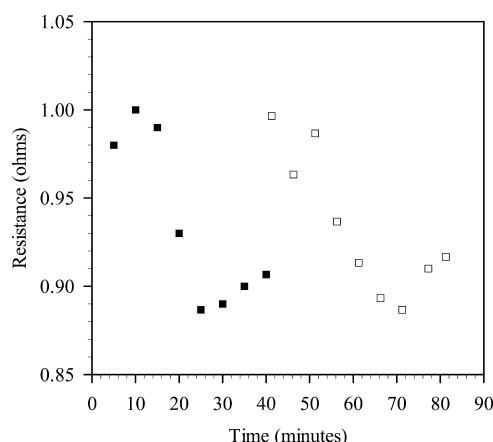
Figure 7. Electrical resistance in succession of two consecutive 40 min polarity cycles at 30 A (612 A/m² current density) as a function of time: (■) polarity B and (□) polarity A.

the electrode that is operating as the cathode in the previous cycle. This reproducible phenomenon after each polarity cycle suggests that the increase in electrical resistance in the module is a function of mineral deposition (scaling).

From the electrical resistance data at the higher applied module current of 30 A (Figures 6 and 7), an empirical module factor of 900 A·min was ascertained by multiplying the applied current by the time in which signs of hardness and scaling on the cathode were observed at that applied current (30 A × 30 min = 900 A·min). This factor is a function of the electrode area and can be used to estimate operating time guidelines for the module at any applied current as shown in eq 2 and listed in Table 1.

$$\text{operational time, min} = (900 \text{ A·min})/(\text{applied current, A}) \tag{2}$$

Table 1. E-CEM Theoretical Operating Parameters

appl curr (A)	oper time (min)	calcd H₂ generation cathode (mL/min)	calcd CO₂ generation (mL/min)
2	450	14	28
4	225	28	55
6	150	42	83
8	113	55	83
10	90	69	83
12	75	83	83
14	64	97	83
16	56	111	83
18	50	125	83
20	45	138	83
22	41	152	83
24	38	166	83
26	35	180	83
28	32	194	83
30	30	208	83

The data in Figures 6 and 7 suggest that the theoretical operational times in Table 1 for an applied module current are realistic. They also suggest that the pH profile during these operational times may be improved by future system and module design changes. These changes include altering the electrode compartment configuration by reducing or eliminating the ion exchange material in the compartment. This could

result in faster equilibrium conditions upon polarity reversal and improved current efficiencies.

NRL has recently reported from laboratory feasibility tests that seawater more readily degasses at pH ≤6 from seawater solutions higher in salt concentration (seawater salinity) and carbonate concentration.[8,9] The studies also suggest that, at higher seawater flow rates, vacuum assisted degassing of CO₂ is required and sample volume and applied vacuum conditions are relevant. Figure 8 illustrates the percent removal of $[CO_2]_T$
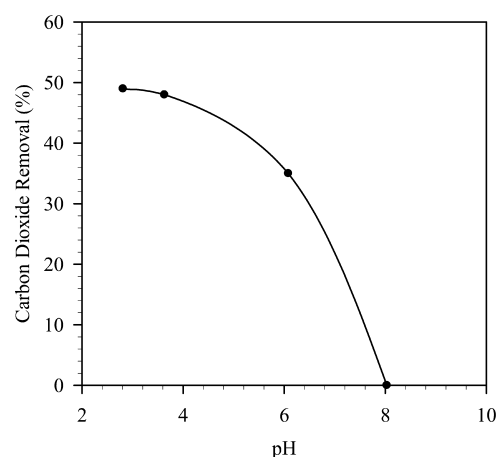

Figure 8. Carbon dioxide removal as a function of pH for effluent seawater samples taken during a 40 min polarity cycle at 20 A (408 A/m² current density), before the gas stripper column.

from seawater plotted as a function of pH during a 20 A, 40 min polarity cycle. In these studies $[CO_2]_T$ removal from the acidified seawater was measured by coulometry. The plot shows that natural Key West seawater was degassed by 46% at effluent seawater pH 4.1 compared to the 30% achieved in the laboratory test module previously reported.[9] When the effluent acidified seawater was passed through a CO₂ vacuum tower and degassed by a 600 mL/min vacuum pump operating at 40 kPa, no measurable improvements in the recovery of CO₂ from the seawater at pH ≤6 were observed. In efforts to increase the effluent seawater surface area during vacuum degassing, two additional larger diameter vacuum towers were constructed from PVC material and tested. Throughout the testing of these columns no measurable improvements in CO₂ recovery were observed over the original vacuum tower design.

A Liqui-Cel polyethylene hollow fiber membrane contactor was tested as another method to increase seawater surface area and thus increase CO₂ recovery from seawater at pH ≤6. Gas permeable membranes are available commercially for the removal or addition of gases from or to liquids. Most of these applications are near atmospheric pressure and include water purification, blood oxygenation, and artificial lung devices.[23−26] However, some are operated at higher pressures such as beverage carbonation.[27,28] It is well-known that these membranes work on the principle of dissolved gases such as carbon dioxide diffusing across the membrane through the pores as a function of differential partial gas pressures. In these experiments, approximately 101 kPa vacuum was applied by a rotary vane vacuum pump to the inside of the hollow fiber membrane tubes in the contactor, as effluent seawater passed over the outside of the membrane fibers at a flow rate of 0.5 gal/min (1900 mL/min).

Figure 9 shows the percent removal of $[CO_2]_T$ plotted as a function of effluent seawater pH for two consecutive 45 min
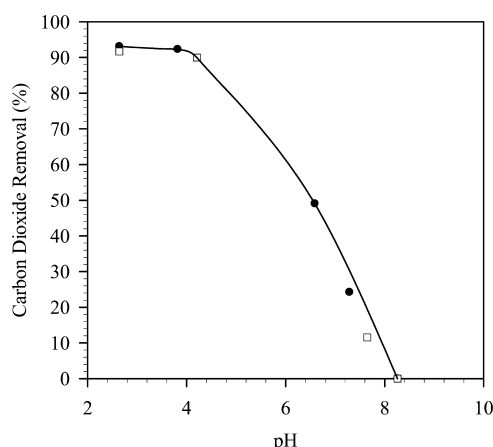

Figure 9. Carbon dioxide removal as a function of pH for effluent seawater samples taken during two consecutive 45 min polarity cycles at 20 A (408 A/m² current density), after contact with hollow fiber membrane contactor.

polarity cycles at 20 A of applied current. From Figure 9, 92% of the CO_2 was removed from the effluent seawater at pH ≤4 at ~101 kPa vacuum. As the effluent seawater pH was lowered further to 2.6, no measurable increase in CO_2 removal was observed. A 92% $[CO_2]_T$ recovery from natural seawater is over 35% more than previously reported using BPMED technology.[19] The lower CO_2 recovery by BPMED is explained by Willauer et al.[8,9]

Similar materials and design were used to construct the hydrogen gas vacuum tower used to separate the H_2 gas from the effluent water stream exiting the electrode compartment acting as the cathode. A 600 mL/min vacuum pump operating at a vacuum of 40 kPa was sufficient to remove the hydrogen gas for real-time detection and analysis by a thermal conductivity detector. At 100% efficiency, the electrode operating as the cathode would produce 222 mL/min H_2. In these studies, the H_2 gas produced at the cathode was analyzed by real-time gas analysis and found to be 85% (v/v) purity. A portion of this gas was captured and independently analyzed by gas chromatographic analysis by TRI Air Testing Inc., which showed 91% (v/v) purity.

The actual energy efficiency of the overall process is limited in this feasibility study by the selection of an off-the-shelf continuous electrodeionization module for modification to an E-CEM. No attempt was made at this point to make the E-CEM (about 49 kWh/m³ H_2 at STP) as energy efficient as a typical commercial water electrolysis unit (about 4.3 kWh/m³ H_2 at STP).[29] This work obtains a total energy of about 11 times this value for hydrogen production. Work is now ongoing to increase the energy efficiencies to achieve parity with commercial water electrolysis H_2. In any event, there is no additional energy cost to simultaneously produce the CO_2 recovered from natural seawater by the E-CEM process. Also, no attempt has yet been made to optimize and minimize the requirement for freshwater use in the functioning electrode compartments. These are all the subject of future work and reports.

CONCLUSIONS

We have described the successful scale-up and characterization of a novel and robust, modified electrolytic cation exchange process (patent pending) for the efficient extraction of CO_2 bound as bicarbonate and carbonate in natural seawater, and the simultaneous production of H_2 gas. We characterized the performance of the process at seawater flows up to 1900 mL/min and demonstrated the ability to extract 92% of $[CO_2]_T$ from natural seawater at pH ≤ 4 under these flow conditions. Electrical resistance profiles suggest that cyclically reversing the polarity of the module's electrodes minimizes the effects of scaling (mineral deposits). In addition, a set of times were ascertained to provide operational parameters for this particular E-CEM. From the pH profiles and the operational conditions, novel module design parameters have been developed to establish faster equilibrium for a future module during polarity reversal and to improve electrical efficiencies. The quantitative production of H_2 at the cathode was measured by real-time thermal conductivity gas analysis and verified independently by gas chromatographic analysis. Finally, while the E-CEM evaluated in these studies is not efficient in energy consumption, these studies have demonstrated the real feasibility of the concept and laid the groundwork needed to pursue custom E-CEM designs that will result in energy efficiencies closer to those currently reported for water electrolysis.

AUTHOR INFORMATION

Corresponding Author
*E-mail: Heather.Willauer@nrl.navy.mil.

Notes
The authors declare no competing financial interest.

ACKNOWLEDGMENTS

REFERENCES

(1) Goeppert, A.; Czaun, M.; Surya Prakash, G. K.; Olah, G. A. Air as the renewable carbon source of the future: an overview of CO_2 capture from the atmosphere. *Energy Environ. Sci.* **2012**, *5*, 7346−7352.

(2) Markewitz, P.; Kuchshinrichs, W.; Leitner, W.; Linssen, J.; Zapp, P.; Bongartz, R.; Schreiber, A.; Müller, T. E. Worldwide innovations in the development of carbon capture technologies and the utilization of CO_2. *Energy Environ. Sci.* **2012**, *5*, 7281−7305.

(3) Takahashi, T.; Broecker, W. S.; Bainbridge, A. E. The Alkalinity and Total Carbon Dioxide Concentration in the World Oceans. In *Carbon Cycle Modelling*; SCOPE: New York, 1981; Vol. *16*, pp 271−286.

(4) Takahashi, T.; Broecker, W. S.; Werner, S. R.; Bainbridge, A. E. Carbonate Chemistry of the Surface of the Waters of the World Oceans. In *Isotope Marine Chemistry*; Goldberg, E. D., Horibe, Y., Katsuko, S., Eds.; Uchida Rokakuho: Tokyo, Japan, 1980; pp 291−326.

(5) Johnson, K. M.; King, A. E.; Sieburth, J. Coulometric TCO₂ Analyses for Marine Studies: An Introduction. *Mar. Chem.* **1985**, *16*, 61.

(6) Coffey, T.; Hardy, D. R.; Besenbruch, G. E.; Schultz, K. R.; Brown, L. C.; Dahlburg, J. P. Hydrogen as a Fuel for DOD. *Def. Horiz.* **2003**, *36*, 1−11.

(7) Willauer, H. D.; Hardy, D. R.; Schultz, K. R.; Williams, F. W. The feasibility and current estimated capital costs of producing jet fuel at

sea using carbon dioxide and hydrogen. *J. Renewable Sustainable Energy* **2012**, *4*, No. 033111.

(8) Willauer, H. D.; DiMascio, F.; Hardy, D. R.; Lewis, M. K.; Williams, F. W. Development of an Electrochemical Acidification Cell for the Recovery of CO_2 and H_2 from Seawater. *Ind. Eng. Chem. Res.* **2011**, *50*, 9876−9882.

(9) Willauer, H. D.; DiMascio, F.; Hardy, D. R.; Lewis, M. K.; Williams, F. W. Development of an Electrochemical Acidification Cell for the Recovery of CO_2 and H_2 from Seawater II. Evaluation of the cell by Natural Seawater. *Ind. Eng. Chem. Res.* **2012**, *51*, 11254−11260.

(10) Prabakaran, P.; Ravindran, A. D. Influence of different carbon and nitrogen sources on growth and CO_2 fixation of microalgae. *Adv. Appl. Sci. Res* **2012**, *3* (3), 1714−1717.

(11) Giordano, M.; Beardall, J.; Raven, J. A. Mechanisms in Algae: Mechanisms, Environmental Modulation, and Evolution. *Annu. Rev. Plant Biol.* **2005**, *56*, 99−131.

(12) Ghasemi, Y.; Rasoul-Amini, S.; Naseri, A. T.; Montazeri-Najagabady, N.; Mobasher, M. A.; Dabbagh, F. Microalgae Biofuel Potentials (Review). *Appl. Biochem. Microbiol.* **2012**, *48*, 126−144.

(13) Fehrenbacher, K. Solidia: Low energy building materials. http://gigaom.com/2011/10/20/solidia-low-energy-building-materials (accessed Jan 7, 2014).

(14) Dorner, R. W.; Hardy, D. R.; Williams, F. W.; Willauer, H. D. C2-C5+ olefin production from CO_2 hydrogenation using ceria modified Fe/Mn/K catalysts. *Catal. Commun.* **2011**, *15*, 88−92.

(15) Dorner, R. W.; Hardy, D. R.; Williams, F. W.; Willauer, H. D. K and Mn doped iron-based CO2 hydrogenation catalysts: Detection of KAlH2 as part of the catalyst's active phase. *Appl. Catal., A: Gen.* **2010**, *373*, 112−121.

(16) Dorner, R. W.; Hardy, D. R.; Williams, F. W.; Willauer, H. D. Heterogeneous catalytic CO_2 conversion to value-added hydrocarbons. *Energy Environ. Sci.* **2010**, *3*, 884−890.

(17) Wang, W.; Wang, S.; Ma, X.; Gong, J. Recent Advances in Catalytic Hydrogenation of Carbon Dioxide. *Chem. Soc. Rev.* **2011**, *40*, 3703−3727.

(18) Centi, G.; Iaquaniello, G.; Perathoner, S. Can We Afford to Waste Carbon Dioxide? Carbon Dioxide as a Valuable Source of Carbon for the Production of Light Hydrocarbons. *ChemSusChem* **2011**, *4*, 1265−1273.

(19) Eisaman, M. D.; Parajuly, K.; Tuganov, A.; Eldershaw, C.; Chang, N.; Littau, K. A. CO2 Extraction from seawater using bipolar membrane electrodialysis. *Energy Environ. Sci.* **2012**, *5*, 7346−7352.

(20) Werner, S.; Morgan, J. J. *Aquatic Chemistry: An Introduction Emphasizing Chemical Equilibrium in Natural Waters*; Wiley-Interscience: New York, 1970.

(21) Katz, W. E. The Electrodialysis Reversal (EDR) Process. *Desalination* **1979**, *28*, 31.

(22) Katz, W. E. Desalination by ED and EDR-State-of-the-Art in 1981. *Desalination* **1982**, *42*, 129.

(23) Bhaumik, D.; Majumdar, S.; Fan, Q.; Sirkar, K. K. Hollow Fiber Membrane Degassing in Ultrapure Water and Microbiocontamination. *J. Membr. Sci.* **2004**, *235*, 31.

(24) Lund, L. W.; Hattler, B. G.; Federspiel, W. J. Gas Permeance Measurement of Hollow Fiber Membranes in Gas-Liquid Environment. *AIChE J.* **2002**, *48*, 635.

(25) Lund, L. W.; Federspiel, W. J.; Hattler, B. G. Gas Permeability of Hollow Fiber Membranes in a Gas-Liquid System. *J. Membr. Sci.* **1996**, *117*, 207.

(26) Eash, H. J.; Jones, H. M.; Hattler, B. G.; Federspiel, W. J. Evaluation of Plasma Resistant Hollow Fiber Membranes for Artificial Lungs. *ASAIO J.* **2004**, *50*, 491.

(27) Bosko, R. S. *Hollow Fiber Carbonation*. U.S. Patent 6,712,342, March 20, 2004.

(28) Gabelman, A.; Hwang, S.-T. Hollow Fiber Membrane Contactors. *J. Membr. Sci.* **1999**, *159*, 61.

(29) NEL Hydrogen. http://www.nel-hydrogen.com/home/ (accessed May 21, 2014).